CP violating phase γ from a global fit of rare charmless hadronic *B* decays

X.-G. He,[1] Y.-K. Hsiao,[1] J.-Q. Shi,[1] Y.-L. Wu,[2] and Y.-F. Zhou[2]
[1]*Department of Physics, National Taiwan University, Taipei, Taiwan*
[2]*Institute of Theoretical Physics, Academia Sinica, Beijing, China*
(Received 28 November 2000; published 15 June 2001)

We study the constraints on the *CP* violating phase γ in the Kobayashi-Maskawa model using available experimental data. We first follow the conventional method to update the constraint on γ by performing a χ^2 analysis using data from $|\epsilon_K|$, $\Delta m_{B_{d,s}}$, and $|V_{ub}/V_{cb}|$. We also include the recent information on $\sin 2\beta$ in the analysis. We obtain the best fit for γ to be 66° and the 95% C.L. allowed range to be 42°–87°. We then develop a method to carry out a χ^2 analysis based on $SU(3)$ symmetry using data from $B\to\pi\pi$ and $B\to K\pi$. We also discuss $SU(3)$ breaking effects from a model estimate. We find that the present data on $B\to\pi\pi, K\pi$ can also give some constraint on γ although weaker than the earlier method limited by the present experimental errors. Future improved data will provide a more stringent constraint. Finally we perform a combined fit using data from $|\epsilon_K|$, $\Delta m_{B_{d,s}}$, $|V_{ub}/V_{cb}|$, $\sin 2\beta$, and rare charmless hadronic *B* decays. The combined analysis gives $\gamma=67°$ for the best-fit value and 43°–87° as the 95% C.L. allowed range. Several comments on other methods to determine γ based on $SU(3)$ symmetry are also provided.

DOI: 10.1103/PhysRevD.64.034002 PACS number(s): 13.20.He, 11.30.Er, 11.30.Hv

I. INTRODUCTION

The origin of *CP* violation is still a mystery although it has been observed in neutral kaon mixing for more than 35 years. One of the most promising models for *CP* violation is the model proposed by Kobayashi and Maskawa in 1973 [1]. This is now referred as the standard model (SM) for *CP* violation. In this model, *CP* violation results from a nonremovable phase γ in the charged current mixing matrix, the Cabibbo-Kobayashi-Maskawa (CKM) matrix [1,2], V_{CKM}. There are also other mechanisms for *CP* violation. To understand the origin of *CP* violation, it is important to study every detail of a particular mechanism against experimental data. In this paper we carry out a study to constrain the *CP* violating phase in the SM using available experimental data.

The CKM matrix V_{CKM} is a 3×3 unitary matrix and is usually written as

$$V_{CKM}=\begin{pmatrix} V_{ud} & V_{us} & V_{ub} \\ V_{cd} & V_{cs} & V_{cb} \\ V_{td} & V_{ts} & V_{tb} \end{pmatrix}. \tag{1}$$

In the literature there are several ways to parametrize the CKM matrix. The standard particle data group parametrization is given by [3]

$$V_{CKM}=\begin{pmatrix} c_{12}c_{13} & s_{12}c_{13} & s_{13}e^{-i\delta_{13}} \\ -s_{12}c_{23}-c_{12}s_{23}s_{13}e^{i\delta_{13}} & c_{12}c_{23}-s_{12}s_{23}s_{13}e^{i\delta_{13}} & s_{23}c_{13} \\ s_{12}s_{23}-c_{12}c_{23}s_{13}e^{i\delta_{13}} & -c_{12}s_{23}-s_{12}c_{23}s_{13}e^{i\delta_{13}} & c_{23}c_{13} \end{pmatrix} \tag{2}$$

where $s_{ij}=\sin\theta_{ij}$ and $c_{ij}=\cos\theta_{ij}$ are the rotation angles. A nonzero value for $\sin\delta_{13}$ violates *CP*. Another commonly used parametrization is the Wolfenstein parametrization [4] which expands the CKM matrix in terms of $\lambda=|V_{us}|$ and is given by

$$V_{CKM}=\begin{pmatrix} 1-\frac{1}{2}\lambda^2 & \lambda & A\lambda^3(\rho-i\eta) \\ -\lambda & 1-\frac{1}{2}\lambda^2 & A\lambda^2 \\ A\lambda^3(1-\rho-i\eta) & -A\lambda^2 & 1 \end{pmatrix} + \mathcal{O}(\lambda^4). \tag{3}$$

The parameters A, ρ, and η are of order unity. When discussing the *CP* violation in a kaon system, it is necessary to keep higher-order terms in λ, namely, adding $-A^2\lambda^5(\rho+i\eta)$ and $-A\lambda^4(\rho+i\eta)$ to V_{cd} and V_{ts}, respectively. The *CP* violation in this parametrization is characterized by a nonzero value for η.

Because of the unitarity condition, one has

$$V_{ub}^*V_{ud}+V_{cb}^*V_{cd}+V_{tb}^*V_{td}=0. \tag{4}$$

In the complex plane the above equation defines a triangle with angles $\alpha=-\mathrm{Arg}(V_{td}V_{tb}^*/V_{ud}V_{ub}^*)$, $\beta=-\mathrm{Arg}(V_{cd}V_{cb}^*/V_{td}V_{tb}^*)$ and $\gamma=-\mathrm{Arg}(V_{ud}V_{ub}^*/V_{cd}V_{cb}^*)$ as shown in Fig. 1.

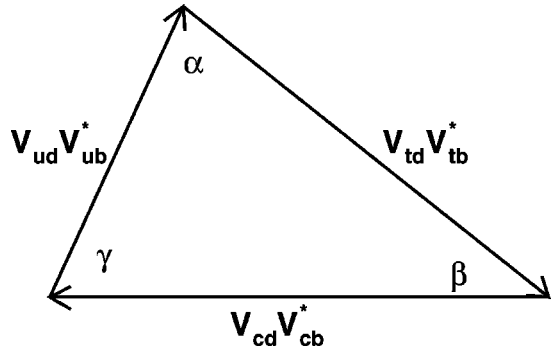

FIG. 1. The KM unitarity triangle.

To a very good approximation the phase δ_{13} is equal to γ. In terms of ρ and η, the angles α, β, and γ are given by

$$\sin 2\alpha = \frac{2\eta(\rho^2-\rho+\eta^2)}{((1-\rho)^2+\eta^2)(\rho^2+\eta^2)},$$

$$\sin 2\beta = \frac{2\eta(1-\rho)}{(1-\rho)^2+\eta^2}, \quad \gamma = \tan^{-1}\frac{\eta}{\rho}. \tag{5}$$

In this paper we will concentrate on obtaining constraint on the phase γ. Great efforts have been made to constrain or to determine the CP violating phase γ. Previous studies mainly used experimental data on (i) the CP violating parameter ϵ_K in the mixing of neutral kaons, (ii) the mixing parameters Δm_{B_d} and Δm_{B_s} in $B_{d,s}-\overline{B}_{d,s}$ systems, and (iii) $|V_{ub}/V_{cb}|$, which characterizes the strength of the charmless flavor changing and charmed flavor changing semileptonic B decays. The best fit value for γ from these considerations is around 65° [5,6].

During the last few years, several rare charmless hadronic B decays have been measured [7]. Some of these decays are sensitive to γ and therefore can be used to constrain it [8,9]. Analysis based on a naive factorization approximation suggests that γ tends to be larger than 90°, in conflict with the analysis mentioned earlier [8,9]. If confirmed, it is an indication of new physics beyond the SM. Of course due to uncertainties in the experimental data and theoretical calculations, it is not possible to draw a firm conclusion as to whether this conflict is real at present. To improve the situation, in this paper we will carry out an analysis replacing the naive factorization assumption by more general $SU(3)$ flavor symmetry for the rare charmless hadronic decays of B to two $SU(3)$ octet pseudoscalars P_1 and P_2, that is, $B \to PP$ decays.

The $SU(3)$ analysis for B decays has been studied by many groups and several interesting results, such as relations between different decay branching ratios, and ways to constrain and/or to determine the phase γ, have been obtained [10–14]. $SU(3)$ symmetry is expected to be a good approximation for B decays. At present, experimental data from $B \to DK(\pi)$ support such an expectation [10]. However, more tests are needed, especially in rare charmless hadronic B decays. Recently it has been shown that such tests can indeed be carried out for rare charmless hadronic B decays in an electroweak model independent way in the future [13]. Before this can be done, however, $SU(3)$ symmetry can only be taken as a working hypothesis. In the rest of the paper we will study constraints that can be obtained from rare charmless hadronic $B \to PP$ decays based on $SU(3)$ symmetry. We will also study $SU(3)$ breaking effects using model calculations.

The paper is arranged as follow. In Sec. II, we will review and update the constraint on γ using information from ϵ_K, $\Delta m_{B_{d,s}}$, and $|V_{ub}/V_{cb}|$, and also information from $\sin 2\beta$ measurement. In Sec. III we will carry out a χ^2 analysis of γ using rare charmless hadronic $B \to PP$ decay data based on $SU(3)$ symmetry. We will also discuss $SU(3)$ breaking effects. In Sec. IV, we will make a combined study using results from Secs. II and III. And in Sec. V, we will discuss some of the implications of the results obtained and draw our conclusions.

II. CONSTRAINT ON γ FROM $|\epsilon_K|$, $\Delta M_{B_{d,s}}$, $|V_{ub}/V_{cb}|$, AND sin2β

In this section we first review and update the constraint on γ using experimental and theoretical information on ϵ_K, $\Delta m_{B_{d,s}}$, and $|V_{ub}/V_{cb}|$. Such an analysis has been carried out before. The analysis in this section is an update of the previous analyses, which also serves to set up our notations for later use. We then include experimental data from the $\sin 2\beta$ measurement into the analysis to obtain the best-fit value and allowed range for γ.

There exist quite a lot of information about the CKM matrix [3]. The value of V_{us} is known from K_{l3} decay and hyperon decays with good precision:

$$\lambda = 0.2196 \pm 0.0023.$$

The parameter A depends on λ and on the CKM matrix element $|V_{cb}|$. Using experimental data from $B \to \overline{D}^* l^+ \nu$ and $B \to \overline{D} l^+ \nu$ and inclusive $b \to c l \overline{\nu}$, analysis from LEP data obtains $V_{cb} = 0.0402 \pm 0.0019$, and data from CLEO obtains $V_{cb} = 0.0404 \pm 0.0034$. The central values of these two measurements are close to each other. In our analysis we will use the averaged value that leads to $A = 0.835 \pm 0.034$.

The value for $|V_{ub}|$ has also been studied using data from $B \to \pi l \overline{\nu}_l$, $B \to \rho l \overline{\nu}_l$, and inclusive $b \to u l \overline{\nu}_l$ with

$$|V_{ub}/V_{cb}| = \lambda\sqrt{\rho^2+\eta^2} = 0.090 \pm 0.025. \tag{6}$$

To separately determine ρ and η (or γ), one has to use information from other data. In the rest of this section we will carry out a χ^2 analysis using constraints from the measurements of $|\epsilon_K|$, $\Delta m_{B_{d,s}}$ and $|V_{ub}/V_{cb}|$ along with other known experimental and theoretical information.

The parameter ϵ_K indicates CP violation in neutral kaon mixing. The short- and long-lived mass eigenstates K_S and

K_L of the neutral kaons can be expressed as the linear combination of weak interaction eigenstates K^0 and $\overline{K^0}$ as $|K_S\rangle = p|K^0\rangle + q|\overline{K^0}\rangle$ and $|K_L\rangle = p|K^0\rangle - q|\overline{K^0}\rangle$. p and q are related to the CP violating parameter ϵ_K in K_L decays by

$$\frac{p}{q} = \frac{1+\epsilon_K}{1-\epsilon_K}. \tag{7}$$

The precise measurements of the $K_S \to \pi\pi$ and $K_L \to \pi\pi$ decay rates imply [3]

$$|\epsilon_K| = (2.271 \pm 0.017) \times 10^{-3}.$$

Evaluating the so-called ''box'' diagram, one obtains

$$|\epsilon_K| = \frac{G_F^2 f_K^2 m_K m_W^2}{6\sqrt{2}\pi^2 \Delta m_K} B_K (A^2\lambda^6\eta)\{y_c[\eta_{ct} f_3(y_c, y_t) - \eta_{cc}] + \eta_{tt} y_t f_2(y_t) A^2\lambda^4(1-\rho)\}. \tag{8}$$

where $\eta_{tt} = 0.574 \pm 0.004$, $\eta_{ct} = 0.47 \pm 0.04$ and $\eta_{cc} = 1.38 \pm 0.53$ [15] are the QCD correction factors, $\Delta m_K = m_{K_L} - m_{K_S} = (0.5300 \pm 0.0012) \times 10^{-2} \mathrm{ps}^{-1}$, and $B_K = 0.94 \pm 0.15$ [16] is the bag factor. The functions f_2 and f_3 of the variables $y_t = m_t^2/m_W^2$ and $y_c = m_c^2/m_W^2$ are given by [17]

$$f_2(x) = \frac{1}{4} + \frac{9}{4(1-x)} - \frac{3}{2(1-x)^2} - \frac{3x^2 \ln x}{2(1-x)^3},$$

$$f_3(x,y) = \ln\frac{y}{x} - \frac{3y}{4(1-y)}\left(1 + \frac{y \ln y}{1-y}\right). \tag{9}$$

Neutral mesons B_d^0 and $\overline{B_d^0}$ show a behavior similar to neutral kaons. The heavy- and light-mass eigenstates, B_L and B_H, are different from B_d^0 and $\overline{B_d^0}$, and are given by

$$|B_L\rangle = p|B_d^0\rangle + q|\overline{B_d^0}\rangle,$$

$$|B_H\rangle = p|B_d^0\rangle - q|\overline{B_d^0}\rangle. \tag{10}$$

The mass difference $\Delta m_{B_d} = m_{B_H} - m_{B_L}$ can be measured by means of the study of the oscillations of one CP eigenstate into the other. The world average value for Δm_{B_d} is [18]

$$\Delta m_{B_d} = 0.487 \pm 0.014 \ \mathrm{ps}^{-1}. \tag{11}$$

The contribution to Δm_{B_d} is from analogous ''box'' diagrams as for ϵ_K, but with the dominant contribution from the top quark in the loop. One obtains

$$\Delta m_{B_d} = \frac{G_F^2}{6\pi^2} m_W^2 m_{B_d} (f_{B_d}\sqrt{B_{B_d}})^2 \eta_B y_t f_2(y_t) A^2\lambda^6 \times [(1-\rho)^2 + \eta^2], \tag{12}$$

where $f_{B_d}\sqrt{B_{B_d}} = 0.215 \pm 0.040$ GeV [19], $\eta_B = 0.55 \pm 0.01$ [15], and the function f_2 is given by Eq. (9).

B_s^0 and $\overline{B_s^0}$ mesons are believed to undergo a mixing analogous to the B_d^0 and $\overline{B_d^0}$. Their larger mass difference Δm_{B_s} is responsible for oscillations that are faster than the B_d^0 and $\overline{B_d^0}$ oscillation, and have thus still eluded direct observation. A lower limit has been set by the CERN e^+e^- collider LEP, SLAC Large Detector and Collider Detector at Fermilab (CDF) Collaborations, as [18]

$$\Delta m_{B_s} > 14.9 \ \mathrm{ps}^{-1} \ (95\% \ \mathrm{C.L.}). \tag{13}$$

The expression for Δm_{B_s} in the SM is similar to that for Δm_{B_d}. Δm_{B_s} can be written as

$$\Delta m_{B_s} = \Delta m_{B_d} \frac{1}{\lambda^2} \frac{m_{B_s}}{m_{B_d}} \xi^2 \frac{1}{(1-\rho)^2 + \eta^2}, \tag{14}$$

where all the theoretical uncertainties are included in a quantity ξ, which is given by [19]

$$\xi = \frac{f_{B_s}\sqrt{B_{B_s}}}{f_{B_d}\sqrt{B_{B_d}}} = 1.14 \pm 0.06. \tag{15}$$

The ρ and η parameters can be determined from a fit to the experimental values of the observables described in the above. In the analysis we will adopt the strategies used in previous analysis in the literature fixing the known parameters, theoretical or experimental, to their central values if their errors were reasonably small as reported in the left-half of Table I. The quantities affected by large errors will be used as additional parameters of the fit, but including a constraint on their value as shown in the right-half of Table I. All errors will be assumed to be Gaussian. This assumption may result in stringent constraints, more than ours actually can be achieved, because some of the errors may obey different distributions, for example, those errors that come from theoretical estimates may obey a flat distribution. Nevertheless, the results provide a good indication for the values of the parameters involved.

To obtain the best-fit values and certain confidence level allowed ranges for the relevant parameters, we perform a χ^2 analysis using the above information. The procedure for χ^2 analysis here is to minimize the following expression:

TABLE I. Input parameters for χ^2 analysis using data from ϵ_K, $\Delta m_{B_{d,s}}$ and $|V_{ub}/V_{cb}|$.

Fixed values	Ref.	Varied parameters	Ref.
$\lambda = 0.2196 \pm 0.0023$	[3]	$A = 0.835 \pm 0.034$	[3]
$G_F = (1.16639 \pm 0.00001) \times 10^{-5}$ GeV^{-2}	[3]	$\eta_{ct} = 0.47 \pm 0.04$	[15]
$f_K = 0.1598 \pm 0.0015$ GeV	[3]	$\eta_{cc} = 1.38 \pm 0.53$	[15]
$\Delta m_K = (0.5300 \pm 0.0012) \times 10^{-2}$ ps^{-1}	[3]	$\overline{m}_c(m_c) = 1.25 \pm 0.10$ GeV	[3]
$m_K = 0.497\,672 \pm 0.000\,031$ GeV	[3]	$\overline{m}_t(m_t) = 165.0 \pm 5.0$ GeV	[3]
$m_W = 80.419 \pm 0.056$ GeV	[3]	$f_{B_d}\sqrt{B_{B_d}} = 0.215 \pm 0.040$ GeV	[16]
$m_{B_d} = 5.2794 \pm 0.0005$ GeV	[3]	$B_K = 0.94 \pm 0.15$	[16]
$m_{B_s} = 5.3696 \pm 0.0024$ GeV	[3]	$\xi = 1.14 \pm 0.06$	[16]
$\eta_{tt} = 0.574 \pm 0.004$	[15]	$\lvert\epsilon_K\rvert = (2.271 \pm 0.017) \times 10^{-3}$	[3]
$\eta_B = 0.55 \pm 0.01$	[15]	$\Delta m_{B_d} = 0.487 \pm 0.014$ ps^{-1}	[18]
		$\lvert V_{ub}/V_{cb}\rvert = 0.090 \pm 0.025$	[3]

$$
\begin{aligned}
\chi^2 = & \frac{(\hat{A}-A)^2}{\sigma_A^2} + \frac{(\widehat{m_c}-m_c)^2}{\sigma_{m_c}^2} + \frac{(\widehat{m_t}-m_t)^2}{\sigma_{m_t}^2} + \frac{(\widehat{B_K}-B_K)^2}{\sigma_{B_K}^2} \\
& + \frac{(\widehat{\eta_{cc}}-\eta_{cc})^2}{\sigma_{\eta_{cc}}^2} + \frac{(\widehat{\eta_{ct}}-\eta_{ct})^2}{\sigma_{\eta_{ct}}^2} \\
& + \frac{(\widehat{f_{B_d}\sqrt{B_{B_d}}} - f_{B_d}\sqrt{B_{B_d}})^2}{\sigma_{f_{B_d}\sqrt{B_{B_d}}}^2} + \frac{(\hat{\xi}-\xi)^2}{\sigma_\xi^2} \\
& + \frac{(\widehat{|V_{ub}|/|V_{cb}|} - |V_{ub}|/|V_{cb}|)^2}{\sigma_{|V_{ub}|/|V_{cb}|}^2} + \frac{(\widehat{|\epsilon_K|} - |\epsilon_K|)^2}{\sigma_{|\epsilon_K|}^2} \\
& + \frac{(\widehat{\Delta m_{B_d}} - \Delta m_{B_d})^2}{\sigma_{\triangle m_{B_d}}^2} + \chi^2(A(\Delta m_{B_s}), \sigma_A(\Delta m_{B_s})).
\end{aligned}
\tag{16}
$$

The symbols with a hat represent the reference values measured or calculated for given physical quantities, as listed in Table I, while the corresponding σ are their errors. The parameters of the fit are ρ, η, A, m_c, m_t, B_K, η_{ct}, η_{cc}, $f_{B_d}\sqrt{B_{B_d}}$ and ξ.

The inclusion of the Δm_{B_s} data needs some explanation. The experimental data consists of measured values of $\mathcal{A}(\Delta m_{B_s})$ and $\sigma_{\mathcal{A}}(\Delta m_{B_s})$ for various values of Δm_{B_s}, plotted in Fig. 2. To include this data in the fit, for each set of free parameters (A, ρ, η, ξ) we calculate the value of Δm_{B_s} and find the corresponding experimental values of $\mathcal{A}$ and $\sigma_{\mathcal{A}}$ in Fig. 2. A nonzero value of Δm_{B_s} implies that $B_s^0 - \overline{B}_s^0$ is mixing, and, if observed, one should have $\mathcal{A}=1$, otherwise $\mathcal{A}=0$ [20]. We follow Ref. [6] to add to the total χ^2 in Eq. (16) a $\Delta\chi^2$ for the corresponding set of (A, ρ, η, ξ)

$$
\Delta\chi^2 = \chi^2[\mathcal{A}(\Delta m_{B_s}), \sigma_{\mathcal{A}}(\Delta m_{B_s})] = \left(\frac{\mathcal{A}-1}{\sigma_{\mathcal{A}}}\right)^2. \tag{17}
$$

$\mathrm{Exp}[-\Delta\chi^2/2]$ is an indication of how likely a mixing with a given Δm_{B_s} was measured by experiment. The sign of the deviation $\mathcal{A}-1$ should also be carefully treated. Naively the expression of $\Delta\chi^2$ implies that a lower probability is attributed to the Δm_{B_s} values with $\mathcal{A}>1$ with respect to the Δm_{B_s} values having $\mathcal{A}=1$. To avoid this undesired behavior, we follow Ref. [6] to set $\mathcal{A}$ to unity for the range with $\mathcal{A}$ larger than one in Fig. 2.

We have carried out the analysis using data directly from Fig. 2. In this way, the points with $\mathcal{A}$ larger than 1 has a larger $\Delta\chi^2$, but the final results on the best fit and 95% C.L. allowed values of the parameters are very similar to the ones obtained by letting $\mathcal{A}=1$ for the region with $\mathcal{A}>1$ in Fig. 2. However, for the reasons discussed above, we will use the results by setting $\mathcal{A}=1$ for region with $\mathcal{A}>1$.

After ρ and η are determined, it is easy to obtain the values of the angles in the unitarity triangle using the relations in Eq. (5). The best-fit values and the allowed regions

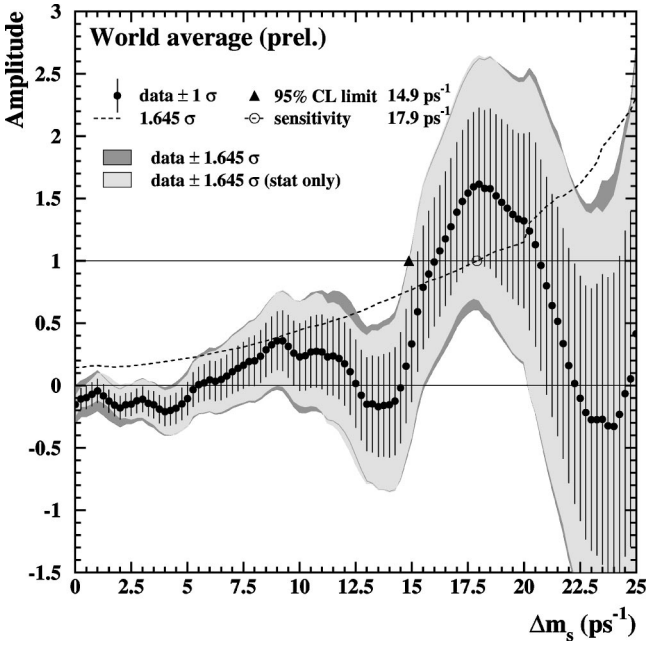

FIG. 2. Experimental data on Δm_{B_s} [17].

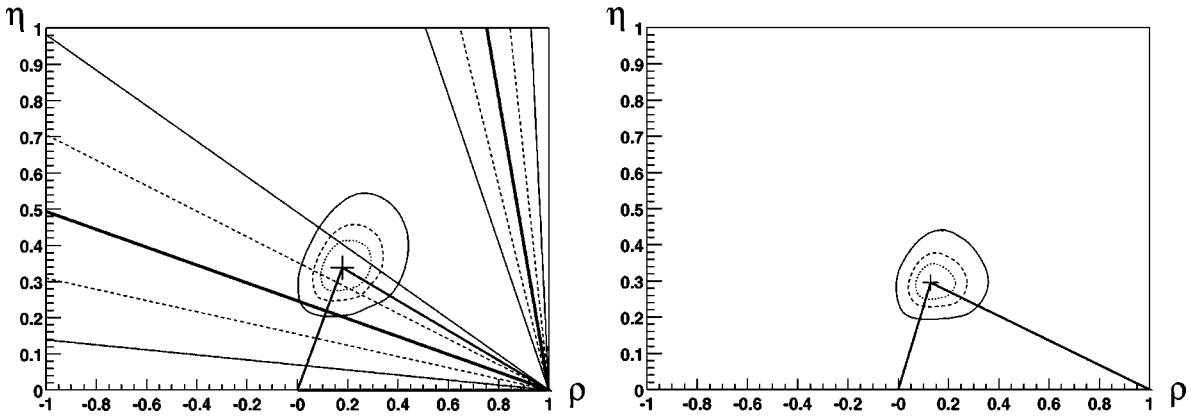

FIG. 3. Constraints on ρ and η using data from $|\epsilon_K|$, $\Delta m_{B_{d,s}}$ and $|V_{ub}/V_{cb}|$, and sin2β. In the figure on the left, only $|\epsilon_K|$, $\Delta m_{B_{d,s}}$, and $|V_{ub}/V_{cb}|$ are used. The best-fit value is indicated by the ''+'' symbol. The region in the dotted curve corresponds to the $\chi^2-\chi^2_{min}=1$ allowed region, which is at the 39% C.L. The 68% C.L. allowed region is within the dashed curve and the 95% C.L. allowed region is within the solid curve. The straight ray lines are the results for the direct measurement of sin2β. The thick solid lines are for the central value of sin2β. There are two allowed regions. The region outside the two thin solid straight lines for each allowed region are excluded by the sin2β measurement at 95% C.L. The 68% C.L. allowed regions are between the dashed lines. The figure on the right is a fit with sin2β data also included in the χ^2.

in the $\rho-\eta$ plane are shown in Fig. 3. The best-fit values and their 68% C.L. errors are

$$\rho=0.18^{+0.11}_{-0.09},\quad \eta=0.34^{+0.07}_{-0.06},$$

$$\sin 2\alpha=-0.19^{+0.37}_{-0.42},\quad \sin 2\beta=0.70^{+0.14}_{-0.09},\quad \gamma=62^{+12^\circ}_{-13^\circ}. \tag{18}$$

The 95% C.L. allowed regions for the above quantities are expressed as

$$0.03<\rho<0.38,\quad 0.23<\eta<0.50,$$

$$-0.85<\sin 2\alpha<0.42,\quad 0.49<\sin 2\beta<0.94,\quad 39^\circ<\gamma<84^\circ. \tag{19}$$

These results agree with previous analyses [5].

The solid line in Fig. 4 is a plot of the minimal χ^2 as a function of γ for the fit using $|\epsilon_K|$, $\Delta m_{B_{d,s}}$ and $|V_{ub}/V_{cb}|$. It is clear that χ^2 changes with γ dramatically. When going away from the minimal, χ^2 raises rapidly indicating a good determination of γ.

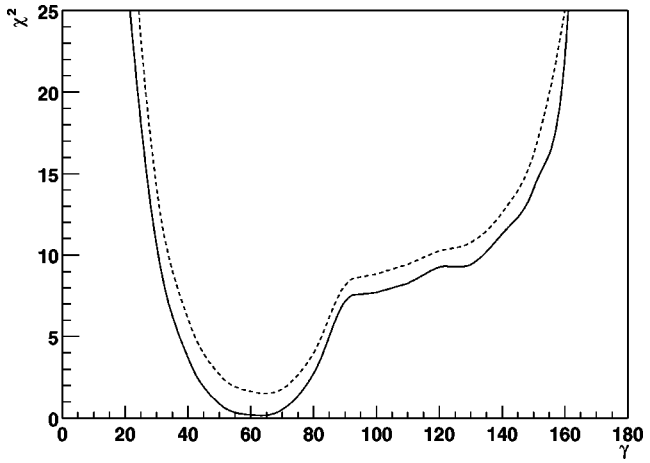

FIG. 4. The solid line is the χ^2 as a function of γ using data from $|\epsilon_K|$, $\Delta m_{B_{d,s}}$ and $|V_{ub}/V_{cb}|$. The dashed line is the χ^2 as a function of γ with sin2β data included in the fit.

There are also direct measurements of $\sin 2\beta$ by several groups from the time-dependent *CP* asymmetry in $B\to J/\psi K_S$. In the SM this asymmetry is given by

$$a(t)=\frac{\Gamma(\overline{B}^0(t)\to J/\psi K_S)-\Gamma(B^0(t)\to J/\psi K_S)}{\Gamma(\overline{B}^0(t)\to J/\psi K_S)+\Gamma(B^0(t)\to J/\psi K_S)} =-\sin 2\beta\sin(\Delta m_{B_d}t). \tag{20}$$

The values measured by different groups are

$$\sin 2\beta=\begin{cases} 0.34\pm 0.20\pm 0.05; & \text{BaBar [21]}\\ 0.58^{+0.32+0.09}_{-0.34-0.10}; & \text{Belle [21]}\\ 0.79^{+0.41}_{-0.44}; & \text{CDF [22]}\\ 0.84^{+0.82}_{-1.04}\pm 0.16 & \text{ALEPH [23].}\end{cases} \tag{21}$$

The averaged value is $\sin 2\beta=0.46\pm 0.16$.

For a given $\sin 2\beta$ there are, in general, four solutions for γ with two of them having negative η and another two having positive η. To determine which one of them is the right solution, one has to use other information. Using the information from our previous fit, we can rule out some of the solutions. The allowed ranges for ρ and η from the averaged value for $\sin 2\beta$ is shown in the figure on the left in Fig. 3 by the straight ray lines. Since the fit from $|\epsilon_K|$, $\Delta m_{B_{d,s}}$ and $|V_{ub}/V_{cb}|$ determines $\eta>0$, only solutions with $\eta>0$ are allowed. It is clear that one of the values for ρ and η, determined from the $\sin 2\beta$ measurement, can be consistent with the fitting results in Eqs. (18) and (19).

It is intersting to note that $\sin 2\beta$ data can eliminate a large allowed range in the ρ vs η plane at the 95% C.L.

level. One can also include the measured $\sin 2\beta$ into the χ^2 analysis. The results are shown in the figure on the right of Fig. 3. The χ^2 as a function of γ is shown by the dashed line in Fig. 4. The best-fit values and their 68% C.L. errors are given by

$$\rho = 0.13^{+0.10}_{-0.06}, \quad \eta = 0.30^{+0.05}_{-0.05},$$
$$\sin 2\alpha = -0.19^{+0.35}_{-0.44}, \quad \sin 2\beta = 0.61^{+0.09}_{-0.07}, \quad \gamma = 66^{+10^\circ}_{-14^\circ}. \tag{22}$$

The 95% C.L. allowed regions for the above quantities are

$$0.01 < \rho < 0.30, \quad 0.21 < \eta < 0.41,$$
$$-0.88 < \sin 2\alpha < 0.45, \quad 0.40 < \sin 2\beta < 0.80, \quad 42^\circ < \gamma < 87^\circ. \tag{23}$$

III. DETERMINATION OF γ FROM CHARMLESS HADRONIC B DECAYS

In this section we study how the phase γ can be constrained from experimental data on $B \to PP$ decays, based on the flavor $SU(3)$ symmetry consideration.

A. The quark level effective Hamiltonian

The quark level effective Hamiltonian, up to one loop level in electroweak interaction for charmless hadronic B decays, including QCD corrections to the matrix elements, can be written as

$$H^q_{eff} = \frac{G_F}{\sqrt{2}}\Bigg[V_{ub}V^*_{uq}(c_1 O_1 + c_2 O_2) - \sum_{i=3}^{11} (V_{ub}V^*_{uq}c_i^{uc} + V_{tb}V^*_{tq}c_i^{tc}) O_i \Bigg]. \tag{24}$$

The coefficients $c_{1,2}$ and $c_i^{jk} = c_i^j - c_i^k$, with j indicating the internal quark, are the Wilson coefficients (WC). These WC's have been evaluated by several groups [24], with $|c_{1,2}| \gg |c_i^j|$. In the above the factor, $V_{cb}V^*_{cq}$ has been eliminated using the unitarity property of the CKM matrix. The operators O_i are defined as [24]

$$O_1 = (\bar{q}_i u_j)_{V-A}(\bar{u}_j b_i)_{V-A}, \quad O_2 = (\bar{q}u)_{V-A}(\bar{u}b)_{V-A},$$
$$O_{3,5} = (\bar{q}b)_{V-A}\sum_{q'} (\bar{q}'q')_{V\mp A},$$
$$O_{4,6} = (\bar{q}_i b_j)_{V-A}\sum_{q'} (\bar{q}'_j q'_i)_{V\mp A},$$
$$O_{7,9} = \frac{3}{2}(\bar{q}b)_{V-A}\sum_{q'} e_{q'}(\bar{q}'q')_{V\pm A},$$
$$O_{8,10} = \frac{3}{2}(\bar{q}_i b_j)_{V-A}\sum_{q'} e_{q'}(\bar{q}'_j q'_i)_{V\pm A}, \tag{25}$$
$$O_{11} = \frac{g_s}{8\pi^2}\bar{q}\sigma_{\mu\nu}G^{\mu\nu}(1+\gamma_5)b,$$

where $(\bar{q}_1 q_2)_{V-A} = \bar{q}_1\gamma_\mu(1-\gamma_5)q_2$, $G^{\mu\nu}$ are the field strengths of the gluon, respectively. We have neglected the photonic dipole penguin term whose contribution to hadronic charmless B decays is small. The usual tree-level W-exchange contribution in the effective Hamiltonian corresponds to O_2. O_1 emerges due to the QCD corrections. The operators $O_{3,4,5,6}$ are from the QCD-penguin diagrams. The operators $O_7, \ldots, O_{10}$ arise from the electroweak-penguin diagrams. O_{11} is the gluonic dipole penguin operator.

The WC's at $\mu = 5$ GeV with $\alpha_s(m_Z) = 0.118$, in the regularization independent scheme in Ref. [25] are

$$c_1 = -0.313, \quad c_2 = 1.150,$$
$$c_3^t = 0.017, \quad c_4^t = -0.037,$$
$$c_5^t = 0.010, \quad c_6^t = -0.046, \tag{26}$$
$$c_7^t = -0.001\alpha_{em}, \quad c_8^t = 0.049\alpha_{em},$$
$$c_9^t = -1.321\alpha_{em}, \quad c_{10}^t = 0.267\alpha_{em}$$
$$c_{11}^t = -0.143,$$

where $\alpha_{em} = 1/128$. $c_i^{c,u}$ are given in Ref. [25]

B. $SU(3)$ Structure of the effective Hamiltonian

To obtain B decay amplitudes, one has to calculate the hadronic matrix elements from quark operators. At present there are no reliable methods to calculate these matrix elements, although simple factorization calculations provide some reasonable results for some decays, but not all of them [26]. It motivates us to carry out model independent analysis by studying properties of the effective Hamiltonian under $SU(3)$ flavor symmetry and use them to obtain information about related decays.

In general the decay amplitudes for $B \to PP$ can be written as

$$A(B \to PP) = \langle PP|H^q_{eff}|B\rangle = \frac{G_F}{\sqrt{2}}[V_{ub}V^*_{uq}T(q) + V_{tb}V^*_{tq}P(q)], \tag{27}$$

where $T(q)$ contains contributions from the *tree* operators $O_{1,2}$, as well as *penguin* operators O_{3-11}, due to charm and up quark loop corrections to the matrix elements, while $P(q)$ contains contributions purely from the *penguin* due to top and charm quarks in loops. The amplitude T in Eq. (27) is usually called the ''tree'' amplitude, which will also be referred to later on in this paper. One should, however, keep in mind that it contains the usual tree current-current contribu-

tions proportional to $c_{1,2}$, and also the u and c penguin contributions proportional to c_i^{uc}, with $i=3-11$. Also, in general, it contains long-distance contributions corresponding to internal u and c generated intermediate hadron states. In our later analysis, we do not distinguish between the tree and the penguin contributions in the amplitude T.

The relative strength of the amplitudes T and P is predominantly determined by their corresponding WC's in the effective Hamiltonian. For $\Delta S=0$ charmless decays, the dominant contributions are due to the tree operators $O_{1,2}$, and the penguin operators are suppressed by smaller WC's. Whereas for $\Delta S=-1$ decays, because the penguin contributions are enhanced by a factor of $V_{tb}V_{ts}^*/V_{ub}V_{us}^*\approx 50$ [3] compared with the tree contributions, penguin effects dominate the decay amplitudes. In this case the electroweak penguins can also play a very important role [27].

The operators $O_{1,2}$, $O_{3-6,11}$, and O_{7-10} transform under $SU(3)$ symmetry as $\bar{3}+\bar{3}'+6+\overline{15}$, $\bar{3}$, and $\bar{3}+\bar{3}'+6+\overline{15}$, respectively. We now give details for the decomposition under $SU(3)$ for some operators. For $\Delta S=0$ decays, O_2 can be written, omitting the Lorentz-Dirac structure, as [13]

$$\begin{aligned}O_2=&-\tfrac{1}{8}\{(\bar{u}u)(\bar{d}b)+(\bar{d}d)(\bar{d}b)+(\bar{s}s)(\bar{d}b)\}_{\bar{3}}+\tfrac{3}{8}\{(\bar{d}u)\\&\times(\bar{u}b)+(\bar{d}d)(\bar{d}b)+(\bar{d}s)(\bar{s}b)\}_{\bar{3}'}-\tfrac{1}{4}\{(\bar{u}u)(\bar{d}b)\\&-(\bar{d}u)(\bar{u}b)+(\bar{d}s)(\bar{s}b)-(\bar{s}s)(\bar{d}b)\}_{6}+\tfrac{1}{8}\{3(\bar{u}u)(\bar{d}b)\\&+3(\bar{d}u)(\bar{u}b)-(\bar{d}s)(\bar{s}b)-(\bar{s}s)(\bar{d}b)-2(\bar{d}d)(\bar{d}b)\}_{\overline{15}}\\=&-\tfrac{1}{8}H(\bar{3})+\frac{3}{8}H(\bar{3}')-\tfrac{1}{4}H(6)+\tfrac{1}{8}H(\overline{15}).\end{aligned}\tag{28}$$

The $\bar{3}$, 6, and $\overline{15}$ indicate the $SU(3)$ irreducible representations. The nonzero entries of the matrices $H(\mathrm{i})$ in flavor space are [10]

$$\begin{aligned}&H(\bar{3})^2=H(\bar{3}')^2=1,\ \ H(6)_1^{12}=H(6)_3^{23}=1,\\&H(6)_1^{21}=H(6)_3^{32}=-1,\\&H(\overline{15})_1^{12}=H(\overline{15})_1^{21}=3,\ \ H(\overline{15})_2^{22}=-2,\\&H(\overline{15})_3^{32}=H(\overline{15})_3^{23}=-1.\end{aligned}\tag{29}$$

Here $1=u$, $2=d$, and $3=s$ with the upper indices indicating antiquarks and the lower ones indicating quarks.

For $\Delta S=1$ decays, one has

$$\begin{aligned}O_2=&-\tfrac{1}{8}\{(\bar{u}u)(\bar{s}b)+(\bar{d}d)(\bar{s}b)+(\bar{s}s)(\bar{s}b)\}_{\bar{3}}+\tfrac{3}{8}\{(\bar{s}u)(\bar{u}b)\\&+(\bar{s}d)(\bar{d}b)+(\bar{s}s)(\bar{s}b)\}_{\bar{3}'}-\tfrac{1}{4}\{(\bar{u}u)(\bar{s}b)-(\bar{s}u)(\bar{u}b)\\&+(\bar{s}d)(\bar{d}b)-(\bar{d}d)(\bar{s}b)\}_{6}+\tfrac{1}{8}\{3(\bar{u}u)(\bar{s}b)+3(\bar{s}u)(\bar{u}b)\\&-(\bar{s}s)(\bar{s}b)-(\bar{s}d)(\bar{d}b)-2(\bar{d}d)(\bar{s}b)\}_{\overline{15}}\\=&-\tfrac{1}{8}H(\bar{3})+\tfrac{3}{8}H(\bar{3}')-\tfrac{1}{4}H(6)+\tfrac{1}{8}H(\overline{15}).\end{aligned}\tag{30}$$

The nonzero entries are [10]

$$\begin{aligned}&H(\bar{3})^3=H(\bar{3}')^3=1,\ \ H(6)_1^{13}=H(6)_2^{32}=1,\\&H(6)_1^{31}=H(6)_2^{23}=-1,\\&H(\overline{15})_1^{13}=H(\overline{15})_1^{31}=3,\ \ H(\overline{15})_3^{33}=-2,\\&H(\overline{15})_2^{32}=H(\overline{15})_2^{23}=-1.\end{aligned}\tag{31}$$

For $\Delta S=0$, the operators $O_{1,2}$, O_{3-6}, and O_{7-10} can be decomposed as

$$\begin{aligned}&O_1=\tfrac{3}{8}\mathcal{O}_{\bar{3}}-\tfrac{1}{8}\mathcal{O}_{\bar{3}'}+\tfrac{1}{4}\mathcal{O}_6+\tfrac{1}{8}\mathcal{O}_{\overline{15}},\\&O_2=-\tfrac{1}{8}\mathcal{O}_{\bar{3}}+\tfrac{3}{8}\mathcal{O}_{\bar{3}'}-\tfrac{1}{4}\mathcal{O}_6+\tfrac{1}{8}\mathcal{O}_{\overline{15}},\\&O_3=\mathcal{O}_{\bar{3}},\qquad O_4=\mathcal{O}_{\bar{3}'},\\&O_9=\tfrac{3}{2}O_1-\tfrac{1}{2}O_3,\ \ O_{10}=\tfrac{3}{2}O_2-\tfrac{1}{2}O_4,\end{aligned}\tag{32}$$

where

$$\begin{aligned}\mathcal{O}_{\bar{3}}=&(\bar{u}u)_{V-A}(\bar{d}b)_{V-A}+(\bar{d}d)_{V-A}(\bar{d}b)_{V-A}\\&+(\bar{s}s)_{V-A}(\bar{d}b)_{V-A},\\\mathcal{O}_{\bar{3}'}=&(\bar{d}u)_{V-A}(\bar{u}b)_{V-A}+(\bar{d}d)_{V-A}(\bar{d}b)_{V-A}\\&+(\bar{d}s)_{V-A}(\bar{s}b)_{V-A},\\\mathcal{O}_6=&(\bar{u}u)_{V-A}(\bar{d}b)_{V-A}-(\bar{d}u)_{V-A}(\bar{u}b)_{V-A}\\&+(\bar{d}s)_{V-A}(\bar{s}b)_{V-A}-(\bar{s}s)_{V-A}(\bar{d}b)_{V-A},\\\mathcal{O}_{\overline{15}}=&3(\bar{u}u)_{V-A}(\bar{d}b)_{V-A}+3(\bar{d}u)_{V-A}(\bar{u}b)_{V-A}\\&-(\bar{d}s)_{V-A}(\bar{s}b)_{V-A}-(\bar{s}s)_{V-A}(\bar{d}b)_{V-A}\\&-2(\bar{d}d)_{V-A}(\bar{d}b)_{V-A}.\end{aligned}\tag{33}$$

The operators O_5 and O_6 have the same $SU(3)$ structure as O_3 and O_4 but different Lorentz-Dirac structures. O_7 and O_8 have the same $SU(3)$ structure as O_9 and O_{10}, but again have different Lorentz-Dirac structures. Similarly one can obtain the decomposition of the operators for $\Delta S=1$ case.

Since we are only concerned with flavor structure in $SU(3)$, operators with different Lorentz-Dirac structures and different color structures can be grouped together according to their flavor $SU(3)$ representations without affecting the results. As long as the flavor structure is concerned, the effective Hamiltonian contains only $\bar{3}$, 6, and $\overline{15}$. These properties enable us to write the decay amplitudes for $B\to PP$ in only a few $SU(3)$ invariant amplitudes.

TABLE II. $SU(3)$ decay amplitudes for $B\to PP$ decays.

$\Delta S=0$	$\Delta S=-1$
$T^{B_u}_{\pi^-\pi^0}(d)=\frac{8}{\sqrt{2}}C^T_{\overline{15}}$,	$T^{B_u}_{\pi^-\bar{K}^0}(s)=C^T_{\overline{3}}-C^T_6+3A^T_{\overline{15}}-C^T_{\overline{15}}$,
$T^{B_u}_{\pi^-\eta_8}(d)=\frac{2}{\sqrt{6}}(C^T_{\overline{3}}-C^T_6+3A^T_{\overline{15}}+3C^T_{\overline{15}})$,	$T^{B_u}_{\pi^0K^-}(s)=\frac{1}{\sqrt{2}}(C^T_{\overline{3}}-C^T_6+3A^T_{\overline{15}}+7C^T_{\overline{15}})$,
$T^{B_u}_{K^-K^0}(d)=C^T_{\overline{3}}-C^T_6+3A^T_{\overline{15}}-C^T_{\overline{15}}$,	$T^{B_u}_{\eta_8K^-}(s)=\frac{1}{\sqrt{6}}(-C^T_{\overline{3}}+C^T_6-3A^T_{\overline{15}}+9C^T_{\overline{15}})$,
$T^{B_d}_{\pi^+\pi^-}(d)=2A^T_{\overline{3}}+C^T_{\overline{3}}+C^T_6+A^T_{\overline{15}}+3C^T_{\overline{15}}$,	$T^{B_d}_{\pi^+K^-}(s)=C^T_{\overline{3}}+C^T_6-A^T_{\overline{15}}+3C^T_{\overline{15}}$,
$T^{B_d}_{\pi^0\pi^0}(d)=\frac{1}{\sqrt{2}}(2A^T_{\overline{3}}+C^T_{\overline{3}}+C^T_6+A^T_{\overline{15}}-5C^T_{\overline{15}})$,	$T^{B_d}_{\pi^0\bar{K}^0}(s)=-\frac{1}{\sqrt{2}}(C^T_{\overline{3}}+C^T_6-A^T_{\overline{15}}-5C^T_{\overline{15}})$,
$T^{B_d}_{K^-K^+}(d)=2(A^T_{\overline{3}}+A^T_{\overline{15}})$,	$T^{B_d}_{\eta_8\bar{K}^0}(s)=-\frac{1}{\sqrt{6}}(C^T_{\overline{3}}+C^T_6-A^T_{\overline{15}}-5C^T_{\overline{15}})$,
$T^{B_d}_{\bar{K}^0K^0}(d)=2A^T_{\overline{3}}+C^T_{\overline{3}}-C^T_6-3A^T_{\overline{15}}-C^T_{\overline{15}}$,	$T^{B_s}_{\pi^+\pi^-}(s)=2(A^T_{\overline{3}}+A^T_{\overline{15}})$,
$T^{B_d}_{\pi^0\eta_8}(d)=\frac{1}{\sqrt{3}}(-C^T_{\overline{3}}+C^T_6+5A^T_{\overline{15}}+C^T_{\overline{15}})$,	$T^{B_s}_{\pi^0\pi^0}(s)=\sqrt{2}(A^T_{\overline{3}}+A^T_{\overline{15}})$,
$T^{B_d}_{\eta_8\eta_8}(d)=\frac{1}{\sqrt{2}}(2A^T_{\overline{3}}+\frac{1}{3}C^T_{\overline{3}}-C^T_6-A^T_{\overline{15}}+C^T_{\overline{15}})$,	$T^{B_s}_{K^+K^-}(s)=2A^T_{\overline{3}}+C^T_{\overline{3}}+C^T_6+A^T_{\overline{15}}+3C^T_{\overline{15}}$,
$T^{B_s}_{K^+\pi^-}(d)=C^T_{\overline{3}}+C^T_6-A^T_{\overline{15}}+3C^T_{\overline{15}}$,	$T^{B_s}_{K^0\bar{K}^0}(s)=2A^T_{\overline{3}}+C^T_{\overline{3}}-C^T_6-3A^T_{\overline{15}}-C^T_{\overline{15}}$,
$T^{B_s}_{K^0\pi^0}(d)=-\frac{1}{\sqrt{2}}(C^T_{\overline{3}}+C^T_6-A^T_{\overline{15}}-5C^T_{\overline{15}})$,	$T^{B_s}_{\pi^0\eta_8}(s)=\frac{2}{\sqrt{3}}(C^T_6+2A^T_{\overline{15}}-2C^T_{\overline{15}})$,
$T^{B_s}_{K^0\eta_8}(d)=-\frac{1}{\sqrt{6}}(C^T_{\overline{3}}+C^T_6-A^T_{\overline{15}}-5C^T_{\overline{15}})$,	$T^{B_s}_{\eta_8\eta_8}(s)=\sqrt{2}(A^T_{\overline{3}}+\frac{2}{3}C^T_{\overline{3}}-A^T_{\overline{15}}-2C^T_{\overline{15}})$.

C. $SU(3)$ decay amplitudes for $B\to PP$ decays

We will use $B_i=(B_u,B_d,B_s)=(B^-,\overline{B}^0,\overline{B}^0_s)$ to indicate the $SU(3)$ triplet for the three B mesons, and M to indicate the pseudoscalar octet M, which contains one of the P in the final state with

$$M=\begin{pmatrix} \frac{\pi^0}{\sqrt{2}}+\frac{\eta_8}{\sqrt{6}} & \pi^+ & K^+ \\ \pi^- & -\frac{\pi^0}{\sqrt{2}}+\frac{\eta_8}{\sqrt{6}} & K^0 \\ K^- & \overline{K}^0 & -2\frac{\eta_8}{\sqrt{6}} \end{pmatrix}. \tag{34}$$

One can write the T amplitude for $B\to PP$ as [10]

$$\begin{aligned} T=&A^T_{\overline{3}}B_iH(\overline{3})^i(M^k_lM^l_k)+C^T_{\overline{3}}B_iM^i_kM^k_jH(\overline{3})^j \\ &+A^T_6B_iH(6)^{ij}_kM^l_jM^k_l+C^T_6B_iM^i_jH(6)^{jk}_lM^l_k \\ &+A^T_{\overline{15}}B_iH(\overline{15})^{ij}_kM^l_jM^k_l+C^T_{\overline{15}}B_iM^i_jH(\overline{15})^{jk}_lM^l_k, \end{aligned} \tag{35}$$

due to the anti-symmetric nature in exchanging the upper two indices of $H^{ij}_k(6)$, and the symmetric structure of the two mesons in the final states, C_6-A_6 always appear together [10]. We will just use C_6 to indicate this combination. There are five complex independent $SU(3)$ invariant amplitudes. The results for each individual B decay mode are shown in Table II. Similarly one can write down the expressions for the penguin induced decay amplitudes P.

Since there are both tree and penguin amplitudes C^T_i, A^T_i and C^P_i, A^P_i, there is, in general, 10 complex hadronic parameters (20 real parameters). However simplications can be made by noticing that $c_{7,8}$ are very small compared with other Wilson coefficients, their contributions can be neglected to a very good precision. In that case, from Eq. (32), we obtain

$$\begin{aligned} C^P_6(A^P_6)&=-\frac{3}{2}\frac{c^{tc}_9-c^{tc}_{10}}{c_1-c_2-3(c^{uc}_9-c^{uc}_{10})/2}C^T_6(A^T_6) \\ &\approx-\frac{3}{2}\frac{c^t_9-c^t_{10}}{c_1-c_2}C^T_6(A^T_6), \end{aligned}$$

$$\begin{aligned} C^P_{\overline{15}}(A^P_{\overline{15}})&=-\frac{3}{2}\frac{c^{tc}_9+c^{tc}_{10}}{c_1+c_2-3(c^{uc}_9+c^{uc}_{10})/2}C^T_{\overline{15}}(A^T_{\overline{15}}) \\ &\approx-\frac{3}{2}\frac{c^t_9+c^t_{10}}{c_1+c_2}C^T_{\overline{15}}(A^T_{\overline{15}}). \end{aligned} \tag{36}$$

We have checked that the approximation signs in the above are good to 10^{-4}.

At the leading order QCD correction, the above relations are renormalization scale independent, and therefore to this order, the coefficients C_i and A_i are also. This can be seen from the fact that when keeping terms that mix only between $O_1(O_9)$ and $O_2(O_{10})$, the dominant QCD correction gives:

$c_{1(9)}(\mu)+c_{2(10)}(\mu)=\eta^{2/\beta}[c_{1(9)}(m_W)+c_{2(10)}(m_W)]$ and $c_{1(9)}(\mu)-c_{2(10)(\mu)}=\eta^{-4/\beta}[c_{1(9)}(m_W)-c_{2(10)}(m_W)]$. Here $c_{1,2,9,10}(m_W)$ are the initial values for the WC's at the W mass scale with $c_{1(10)}(m_W)=0$, $\eta=\alpha_s(m_W)/\alpha_s(\mu)$ and $\beta=11-2f/3$ (f is the number of quark flavors with mass smaller than μ). These relations lead to $[c_9(\mu)\pm c_{10}(\mu)]/[c_1(\mu)\pm c_2(\mu)]=\pm c_9(m_W)/c_2(m_W)$ independent of μ. Mixings with other operators and higher-order corrections introduce dependence on renormalization schemes. We have checked with different renormalization schemes and find that numerically the changes are less than 15% for different schemes. Although the changes are not sizable, there is scheme dependence. The total decay amplitudes are not renormalization scheme dependent, therefore the hadronic matrix elements determined depend on the renormalization scheme used to determine the ratios, $(c_9\pm c_{10})/(c_1\pm c_2)$. One should consistently use the same scheme.

Using relations in Eq. (36), one finds that there are less independent parameters which we choose to be $C_{\bar{3}}^{T,P}(A_{\bar{3}}^{T,P})$, C_6^T, and $C_{\overline{15}}^T(A_{\overline{15}}^T)$. Using the fact that an overall phase can be removed without loss of generality, we will set $C_{\bar{3}}^P$ to be real. There are in fact only 13 real independent parameters for $B\to PP$ in the SM.

One can further reduce the parameters with some dynamic considerations. To this end we note that the amplitudes A_i correspond to annihilation contributions, as can be seen from Eq. (35), where B_i mesons are contracted with one of the indices in $H(j)$, and are small compared with the amplitudes C_i from model calculations and are often neglected in factorization calculations [8,26]. Neglecting all annihilation contributions, we then have just seven independent hadronic parameters in the amplitudes

$$C_{\bar{3}}^P,\quad C_{\bar{3}}^T e^{i\delta_{\bar{3}}},\quad C_6^T e^{i\delta_6},\quad C_{\overline{15}}^T e^{i\delta_{\overline{15}}}. \tag{37}$$

The phases in the above are defined in such a way that all $C_i^{T,P}$ are real positive numbers.

We will make the assumption that annihilation amplitudes are negligibly small in our later analysis and leave the verification of this assumption for future experimental data. We point out that this assumption can be tested using $B_d\to K^-K^+$, $B_s\to\pi^+\pi^-$, and $\pi^0\pi^0$ in $B\to PP$ decays, because these decays have only annihilation contributions as can be seen from Table II [12,13].

D. Constraint on γ from $B\to PP$ decays

We are now ready to carry out a χ^2 analysis using data from $B\to\pi\pi$ and $B\to K\pi$. The experimental data to be used are shown in Table III.

In general the errors for the experimental data in Table III are correlated. Due to the lack of knowledge of the error correlation from experiments, in our analysis, for simplicity, we take them to be uncorrelated and assume the errors obey Gaussian distribution taking the larger one between σ_+ and σ_- to be on the conservative side. When combining from different measurements, we take the weighted average. For the data which only presented as upper bounds, we assume them to obey Gaussian distribution and take the error σ accordingly.

TABLE III. Rare hadronic charmless $B\to\pi\pi$ and $B\to K\pi$ data. The branching ratios are in units of 10^{-6}.

Br and A_{CP}	Data	Value used from combined data
$\mathrm{Br}(B\to\pi^+\pi^-)$	$4.3^{+1.6}_{-1.4}\pm0.5$ [7,28]	4.4 ± 0.9
	$5.9^{+2.4}_{-2.1}\pm0.5$ [29]	
	$4.1\pm1.0\pm0.7$ [30]	
$\mathrm{Br}(B\to\pi^-\pi^0)$	$5.6^{+2.6}_{-2.3}\pm1.7$ [7,28]	6.2 ± 2.4
	$7.1^{+3.6+0.9}_{-3.0-1.2}$ [29]	
$\mathrm{Br}(B\to K^+\pi^-)$	$17.2^{+2.5}_{-2.4}\pm1.2$ [7,28]	17.3 ± 1.6
	$18.7^{+3.3}_{-3.0}\pm1.6$ [29]	
	$16.7\pm1.6^{+1.2}_{-1.7}$ [30]	
$\mathrm{Br}(B\to K^-\pi^0)$	$11.6^{+3.0+1.4}_{-2.7-1.3}$ [7,28]	13.7 ± 2.6
	$17.0^{+3.7+2.0}_{-3.0-2.2}$ [29]	
$\mathrm{Br}(B\to\bar{K}^0\pi^-)$	$18.2^{+4.6}_{-4.0}\pm1.6$ [7,28]	16.2 ± 3.8
	$13.1^{+5.5}_{-4.6}\pm2.6$ [29]	
$\mathrm{Br}(B\to K^0\pi^0)$	$14.6^{+5.9+2.4}_{-5.1-3.3}$ [7,28]	14.6 ± 4.6
	$14.6^{+6.1}_{-5.1}\pm2.7$ [29]	
$\mathrm{Br}(B\to K^-K^0)$	<5.1(90% C.L.) [7,28]	0.6 ± 1.9
	<5.0(90% C.L.) [29]	
$\mathrm{Br}(B\to\pi^0\pi^0)$	$2.1^{+1.7+0.7}_{-1.3-0.6}$ [28]	2.1 ± 1.8
$A_{CP}(B\to K^-\pi^0)$	-0.29 ± 0.23 [31]	-0.13 ± 0.16
	$0.019^{+0.219}_{-0.191}$ [29]	
$A_{CP}(B\to K^+\pi^-)$	-0.04 ± 0.16 [31]	-0.003 ± 0.12
	$0.043\pm0.175\pm0.021$ [29]	
$A_{CP}(B\to\bar{K}^0\pi^-)$	0.18 ± 0.24 [31]	0.18 ± 0.24

The χ^2 analysis in this case is to minimize the χ^2 given as

$$\chi^2=\sum_i\frac{[\hat{B}r(i)-Br(i)]^2}{\sigma_{Br}^2(i)}+\sum_i\frac{[\hat{A}_{CP}(i)-A_{CP}(i)]^2}{\sigma_{CP}^2(i)}+\chi^2(A,|V_{ub}/V_{cb}|), \tag{38}$$

where the summation on i is for the available decay branching ratios and the CP asymmetries are listed in Table III. $\sigma_{Br,CP}$ are the corresponding errors. Here $\chi^2(A,|V_{ub}/V_{cb}|)$ is the χ^2 due to uncertainties in A and $|V_{ub}/V_{cb}|$ in Sec. II. The branching ratios $\mathrm{Br}(i)$ and the CP asymmetries $A_{CP}(i)$, expressed in terms of the decay amplitude $A(i)=(G_F/\sqrt{2})[V_{ub}V_{uq}^*T(i)+V_{tb}V_{tq}^*P(i)]$ for a particular $B\to P_1P_2$, are given by

$$\mathrm{Br}(i)=\frac{1}{32\pi m_B\Gamma_B}(|A(i)|^2+|\bar{A}(i)|^2)\lambda_{P_1P_2},$$

$$A_{CP}(i)=\frac{|A(i)|^2-|\bar{A}(i)|^2}{|A(i)|^2+|\bar{A}(i)|^2}, \tag{39}$$

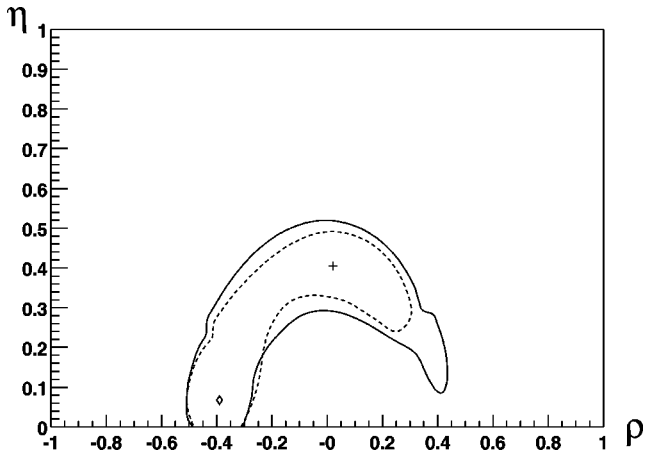

FIG. 5. The constraints for ρ and η using data from $|V_{ub}/V_{cb}|$ and rare $B\to\pi\pi$ and $B\to K\pi$. For the fit with exact $SU(3)$, the best-fit value is indicated by the ''+'' symbol and the $\chi^2-\chi^2_{min}=1$ (39% C.L.) allowed regions are inside the region in the solid curve. For the case with $SU(3)$ breaking effects, the best-fit value is indicated by a diamond shaped symbol and the 39% C.L. allowed region is inside the dashed curve.

where $\lambda_{ij}=\{[1-(m_i+m_j)^2/m_B^2][1-(m_i-m_j)^2/m_B^2]\}^{1/2}$. The amplitudes $T(i)$ and $P(i)$ for each individual decay can be read off from Table II.

We use $V_{cb}=0.0402\pm0.0019$ and $|V_{ub}/V_{cb}|=0.090\pm0.025$ in the fitting. The results with exact $SU(3)$ symmetry are shown in Figs. 5 and 6 by the solid curves. The best fit values for the hadronic parameters are

$$C_{\bar{3}}^P=0.13,\quad C_3^T=0.34,\quad C_6^T=0.13,\quad C_{\overline{15}}^T=0.16,$$

$$\delta_{\bar{3}}=-27^\circ,\quad \delta_6=-20^\circ,\quad \delta_{\overline{15}}=35^\circ. \tag{40}$$

And the best-fit values for ρ, η and γ are

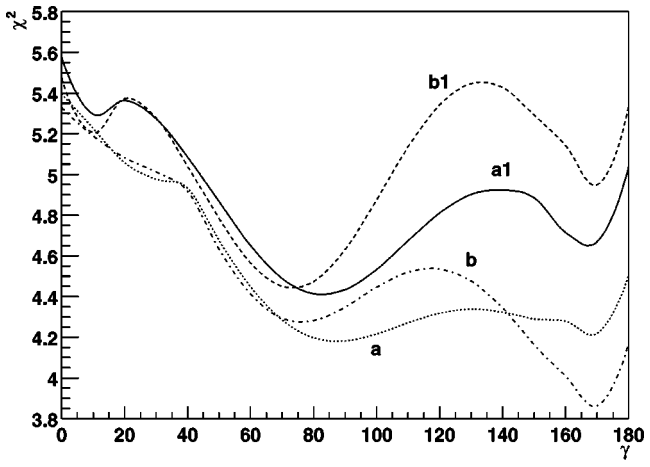

FIG. 6. χ^2 as a function of γ using data from $|V_{ub}/V_{cb}|$ and rare $B\to\pi\pi$ and $B\to K\pi$. The curve (a) is for the case with exact $SU(3)$, and the curve (b) is for the one with $SU(3)$ breaking effects. The curves (a1) and (b1) are for the cases with the additional condition $C_3^T e^{i\delta_{\bar{3}}}-C_6^T e^{i\delta_6}-C_{\overline{15}}^T e^{i\delta_{\overline{15}}}=0$ with exact $SU(3)$ and with $SU(3)$ breaking effects, respectively.

$$\rho=0.02,\quad \eta=0.40,\quad \gamma=87^\circ. \tag{41}$$

The constraint is weak. We have not given the 68% allowed ranges because to that level, the constraints are basically given by $|V_{ub}/V_{cb}|$. We have to wait for more accurate data to obtain a more restrictive constraints.

At present the errors on the asymmetries are too large and do not really provide stringent constraints. However, we include them here hoping that they will be measured soon. By then one can easily include them in the fit to obtain more stringent constraint on γ.

In Fig. 5, we show the regions allowed by $\chi^2-\chi^2_{min}=1$ in the $\rho-\eta$ plane by the solid curve. As mentioned, at present the constraint is weak, which can also be seen from Fig. 6 where the minimal χ^2 as a function of γ is shown by the curve (a) for the case with exact $SU(3)$ symmetry, although the χ^2_{min} per degree of freedom is smaller than 1. The 68% allowed region is actually the same as that from $|V_{ub}/V_{cb}|$ alone. However, when more precision data for rare charmless $B\to PP$ become available, the restriction will become more stringent. For example, if the error bars for all the quantities are reduced by a factor of 2.45, then the regions in Fig. 5 correspond to 95% C.L. allowed regions.

$SU(3)$ may not be an exact symmetry for $B\to PP$. We now estimate $SU(3)$ breaking effects. The amplitudes C_i for $B\to\pi\pi$ and $B\to K\pi$ will be different if $SU(3)$ is broken. At present it is not possible to calculate the breaking effects. To have some idea about the size of the $SU(3)$ breaking effects, we work with the factorization estimate. To leading order, the relation between the amplitudes for $B\to\pi\pi$ decays $C_i(\pi\pi)$ and the amplitudes for $B\to K\pi$ decays $C_i(K\pi)$, can be parametrized as $C_i(K\pi)=rC_i(\pi\pi)$, and r is approximately given by

$$r\approx\frac{f_K}{f_\pi}=1.22. \tag{42}$$

Here we have assumed that the $SU(3)$ breaking effects in f_i and $F_0^{B\to i}$ are similar in magnitudes, that is, $f_K/f_\pi\approx F_0^{B\to K}/F_0^{B\to\pi}$ [32]. Using the above to represent the $SU(3)$ breaking effect, we can obtain another set of fitting results. They are shown in Figs. 5 (dashed curve) and 6 [curve (b)]. The best-fit values for the amplitudes are

$$C_{\bar{3}}^P=0.11,\quad C_3^T=0.33,\quad C_6^T=0.22,\quad C_{\overline{15}}^T=0.18,$$

$$\delta_{\bar{3}}=57^\circ,\quad \delta_6=200^\circ,\quad \delta_{\overline{15}}=85^\circ. \tag{43}$$

The best-fit values for ρ, η and γ are given by

$$\rho=-0.39,\quad \eta=0.07,\quad \gamma=170^\circ. \tag{44}$$

In both exact and broken $SU(3)$ cases, there are two local minimum in the χ^2 vs γ diagrams. The corresponding values of γ are very different with one of them around 87° and another 170°. These best-fit values are dramatically different than those obtained in Sec. II. However, the best-fit values here can not be taken too seriously because, as can be seen from Fig. 5, at the 39% C.L. level, almost all allowed ranges

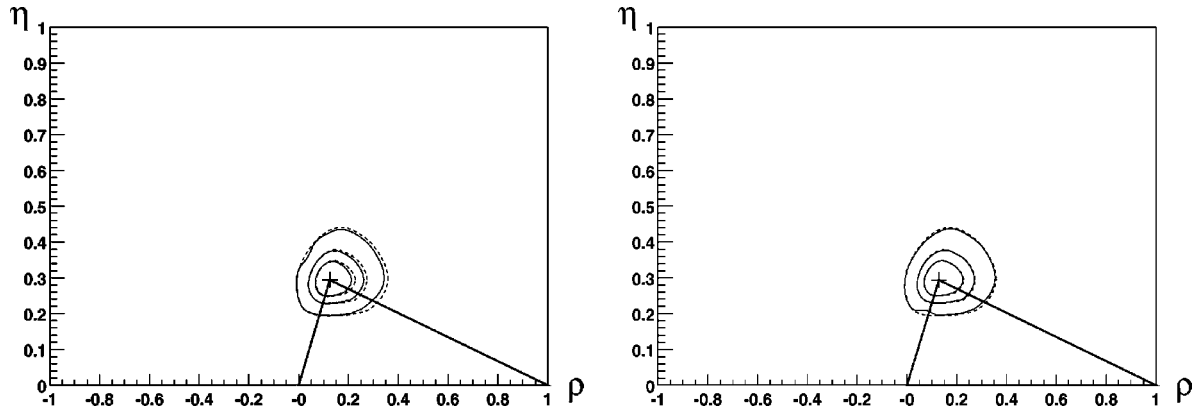

FIG. 7. Constraints on ρ and η using combined data from $|\epsilon_K|$, $\Delta m_{B_{d,s}}$, $|V_{ub}/V_{cb}|$, sin2β, and $B\to\pi\pi$ and $B\to K\pi$. The three regions, from smaller to larger, corresponds to the $\chi^2-\chi^2_{min}=1$ allowed region, which is at the 39% C.L., the 68% C.L. allowed region, and the 95% C.L. allowed region, respectively. The figure on the left is for the case with exact $SU(3)$ and the one on the right is for the case with $SU(3)$ breaking effects. The dotted curves are for fit in Sec. II and the solid curves are for the combined fit.

by $|V_{ub}/V_{cb}|$ are allowed by $B\to PP$ data. At the 68% C.L. level, all allowed regions by $|V_{ub}/V_{cb}|$ are allowed by data from the $B\to PP$ decays. Inconsistence between γ obtained in Sec. II and this section cannot be established. We have to wait for more precise data on $B\to PP$ to decide.

In the literature it has often been quoted that $O_{1,2}$ do not contribute to $B^-\to\overline{K}^0\pi^-$, and therefore $\mathrm{Br}(B^-\to\overline{K}^0\pi^-)=\mathrm{Br}(B^+\to K^0\pi^+)$. In the $SU(3)$ language used here, this implies $C=C_{\overline{3}}^T e^{i\delta_{\overline{3}}}-C_6^T e^{i\delta_6}-C_{\overline{15}}^T e^{i\delta_{\overline{15}}}=0$. This result has been used to derive several methods to determine the phase γ. We stress that this is not a result from the $SU(3)$ consideration and needs to be checked. For this reason, we also carried out analyses with the condition $C=0$. For this case, the minimal χ^2 as a function of γ, are also shown in Fig. 6 [curves (a1) and (b1)] with exact $SU(3)$ and with $SU(3)$ breaking effects, respectively. The best-fit values with exact $SU(3)$ symmetry are

$$\rho=0.05,\quad \eta=0.41,\quad \gamma=83^\circ,$$

$$C_{\overline{3}}^P=0.13,\quad C_{\overline{3}}^T=0.26,\quad C_6^T=0.17,\quad C_{\overline{15}}^T=0.16,$$

$$\delta_{\overline{3}}=-13^\circ,\quad \delta_6=-49^\circ,\quad \delta_{15}=27^\circ. \tag{45}$$

And the best-fit values with $SU(3)$ breaking effects are

$$\rho=0.12,\quad \eta=0.39,\quad \gamma=73^\circ,$$

$$C_{\overline{3}}^P=0.11,\quad C_{\overline{3}}^T=0.24,\quad C_6^T=0.15,\quad C_{\overline{15}}^T=0.16,$$

$$\delta_{\overline{3}}=-15^\circ,\quad \delta_6=-56^\circ,\quad \delta_{\overline{15}}=23^\circ. \tag{46}$$

The imposition of $C=0$ does not force these coefficients to be real. In order to get C to be zero, the real and imaginary parts both have to cancel to satisfy the condition. The implications of this analysis will be discussed later.

IV. COMBINED FIT

In this section we carry out a combined fit of Secs. II and III. The total $\chi^2(total)$ is the sum of the χ^2(II) with the $\sin 2\beta$ data included from Sec. II plus the χ^2(III). Here χ^2(III) is the χ^2 in Eq. (36) of Sec. III with $\chi^2(A,|V_{ub}/V_{cb}|)$ subtracted. This is because χ^2(II) already includes information from A and $|V_{ub}/V_{cb}|$. The results are shown in Figs. 7 and 8. Since χ^2(II) has a sharper dependence on γ compared with χ^2(III), the best-fit values and errors are dominantly determined by constraints in Sec. II.

The best combined fit values with exact $SU(3)$ symmetry for the hadronic parameters are

$$C_{\overline{3}}^P=0.13,\quad C_{\overline{3}}^T=0.29,\quad C_6^T=0.16,\quad C_{\overline{15}}^T=0.20,$$

$$\delta_{\overline{3}}=-42^\circ,\quad \delta_6=-20^\circ,\quad \delta_{\overline{15}}=35^\circ. \tag{47}$$

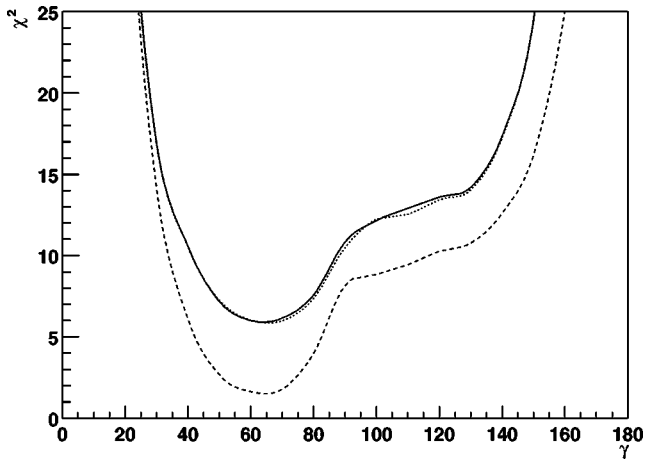

FIG. 8. χ^2 as a function of γ using combined data from $|\epsilon_K|$, $\Delta m_{B_{d,s}}$, $|V_{ub}/V_{cb}|$, $\sin 2\beta$, and rare $B\to PP$ data. The dotted and solid curves are for the fit with exact $SU(3)$ and with $SU(3)$ breaking effects, respectively. The dashed curve is the same as that from Sec. II with $\sin 2\beta$ included.

In the above, we have not given errors for the hadronic parameters because the constraints on them are weak.

The best-fit values for ρ, η, and γ and their 68% C.L. errors are given by

$$\rho=0.12^{+0.09}_{-0.05},\quad \eta=0.29^{+0.06}_{-0.04},\quad \gamma=67^{+10^\circ}_{-13^\circ}, \tag{48}$$

and the 95% C.L. allowed ranges for ρ, η, and γ are

$$\begin{aligned} &0.01<\rho<0.29,\quad 0.21<\eta<0.40,\\ &-0.86<\sin 2\alpha<0.45,\quad 0.45<\sin 2\beta<0.79,\\ &43^\circ<\gamma<87^\circ. \end{aligned} \tag{49}$$

The best combined fit values with $SU(3)$ breaking effects for the hadronic parameters are

$$\begin{aligned} &C_{\bar 3}^P=0.11,\quad C_3^T=0.29,\quad C_6^T=0.16,\quad C_{\overline{15}}^T=0.20,\\ &\delta_{\bar 3}=-33^\circ,\quad \delta_6=-40^\circ,\quad \delta_{\overline{15}}=31^\circ, \end{aligned} \tag{50}$$

$$\rho=0.13^{+0.09}_{-0.06},\quad \eta=0.29^{+0.06}_{-0.04},\quad \gamma=66^{+10^\circ}_{-13^\circ}, \tag{51}$$

and the 95% C.L. allowed ranges for ρ, η, and γ are

$$\begin{aligned} &0.01<\rho<0.30,\quad 0.21<\eta<0.41,\\ &-0.87<\sin 2\alpha<0.44,\quad 0.46<\sin 2\beta<0.80,\\ &42^\circ<\gamma<87^\circ. \end{aligned} \tag{52}$$

V. DISCUSSIONS AND CONCLUSIONS

At present, the rare charmless hadronic B decay data have large error bars. The main contribution to the χ^2 for the analysis in Secs. III and IV, come from the branching ratio for $\overline{B}^0\to\overline{K}^0\pi^0$. In the cases discussed, this mode alone contributes about 2.5 to the χ^2. The best-fit value of the branching ratio is only about half of the experimental central value. We suspect that there may be some systematic errors in the measurement of this branching ratio. If the present central value persists, it may be an indication of badly broken $SU(3)$ symmetry or new physics beyond the SM. It is important to improve the precision of experimental data to decide whether new physics is needed.

Because of the large error bars associated with the $B\to PP$ data, the ranges determined for the related parameters have large error bars. The γ phase has a large range allowed by using the $B\to PP$ data alone. However, the fit shows no conflict between the fit from the consideration using $|\epsilon_K|$, $\Delta m_{B_{d,s}}$, $|V_{ub}/V_{cb}|$ and $\sin 2\beta$ data. Future experimental data will be able to provide a more accurate determination of the γ phase.

Before closing we would like to make a few comments about our analysis and some other related calculations. Our first comment concerns the general $SU(3)$ analysis and factorization calculations.

Assuming factorization and the $SU(3)$ symmetry, that is the decay constants for all octet pseudoscalars P are equal, and the form factors for $B\to P$ are also equal, one obtains [26]

$$\begin{aligned} C_{\bar 3}^T&=\left\{\frac{3a_2-a_1}{8}-\left[(a_4^{uc}+a_6^{uc}R)+\frac{3}{16}(a_7^{uc}-a_9^{uc})\right.\right.\\ &\left.\left.+\frac{1}{16}(a_{10}^{uc}+a_8^{uc}R)\right]\right\}X,\\ C_6^T&=\left\{\frac{a_2-a_1}{4}-\frac{3}{8}(a_{10}^{uc}-a_9^{uc}+a_7^{uc}+a_8^{uc}R)\right\}X,\\ C_{\overline{15}}^T&=\left\{\frac{a_1+a_2}{8}-\frac{3}{16}(a_9^{uc}+a_{10}^{uc}-a_7^{uc}+a_8^{uc}R)\right\}X, \end{aligned} \tag{53}$$

where

$$X=f_\pi F_0^{B\to\pi}(m_\pi^2)(m_B^2-m_\pi^2)$$

and

$$R=m_K^2/(m_b-m_q)(m_s+m_q).$$

These amplitudes are related to the ''tree'' contributions, $a_i^{uc}=a_i^u-a_i^c$ with $a_{2i}=c_{2i}+c_{2i-1}/N$ and $a_{2i-1}=c_{2i-1}+c_{2i}/N$.

The penguin amplitudes are given by [26]

$$\begin{aligned} C_{\bar 3}^P&=-[(a_4^{tc}+a_6^{tc}R)+\tfrac{3}{16}(a_7^{tc}-a_9^{tc})+\tfrac{1}{16}(a_{10}^{tc}+a_8^{tc}R)]X,\\ C_6^P&=-\tfrac{3}{8}(a_{10}^{tc}-a_9^{tc}+a_7^{tc}+a_8^{tc}R)X,\\ C_{\overline{15}}^P&=-\tfrac{3}{16}(a_9^{tc}+a_{10}^{tc}-a_7^{tc}+a_8^{tc}R)X, \end{aligned} \tag{54}$$

where $a_i^{tc}=a_i^t-a_i^c$. When small contributions from $a_{7,8}^{ij}$ terms are neglected, one recovers the relations in Eq. (36). Numerically, we have

$$\begin{aligned} &C_{\bar 3}^P=0.09,\quad C_3^T=0.42,\quad C_6^T=0.26,\quad C_{\overline{15}}^T=0.15,\\ &\delta_{\bar 3}=-15.7^\circ,\quad \delta_6=-14.5^\circ,\quad \delta_{\overline{15}}=-14.5^\circ. \end{aligned} \tag{55}$$

In the above we have used the convention with $C_{\bar 3}^P$ to be real.

The amplitudes are in the same order of magnitude as the best-fit values in Secs. III and IV, but the phase can be very different. In the factorization approximation calculation here, phases are only due to short-distance interaction, rescattering of quarks. Long-distance contributions can change these phases. The results of the best-fit values for the phases indicate that there may be large long-distance rescattering effects.

Our second comments concern the combination of the $SU(3)$ invariant decay amplitude $C=C_{\bar 3}^T e^{i\delta_{\bar 3}}-C_6^T e^{i\delta_6}-C_{\overline{15}}^T e^{\delta_{\overline{15}}}$. It has been usually assumed in the literature that $C=0$. This leads to $\mathrm{Br}(B^+\to K^0\pi^+)=\mathrm{Br}(B^-\to\overline{K}^0\pi^-)$. This result played a crucial role in several methods to con-

strain and to determine the phase γ, for example, using [9] $B^- \to K^- \pi^0$, $\overline{K^0}\pi^-, \pi^-\pi^-$, $\overline{B^0}(B^-) \to K^+\pi^-$, $\pi^+\pi^-(\overline{K^0}\pi^-)$, and $B^- \to K^-\pi^0, \overline{K^0}\pi^-, K^-\eta$.

We point out that $C=0$ is based on the factorization calculation neglecting annihilation contributions and also penguin contributions [26]. In fact, using factorization calculations when penguin contributions are included, C does not equal zero, but $C = C_3^T(\text{penguin})$. $C_3^T(\text{penguin})$ can be obtained from Eq. (53) (the terms proportional to c_i^{uc} in C_3^T). In the factorization framework, we can easily check whether $C=0$ is a good approximation. Using the result in Eq. (53), we find that the $|C_3^T(\text{penguin})/C_3^T|$ is of order 5%. It is therefore reasonable to assume the penguin contribution to be small and $C \approx 0$.

One should also be aware that when going beyond factorization approximation and include rescattering effects, C may deviate from zero, however, it should be tested. The fitting program proposed in this paper can be easily used to achieve this goal. From the best-fit values in the previous sections, we clearly see that C can easily deviate from zero. For example, in the case with exact $SU(3)$, the best-fit value using rare B decay data C is $C = 0.05 - i0.20$, and with $SU(3)$ breaking effects C is $C = 0.37 + i0.18$, which are the same order of magnitude as individual C_i^T. One needs more data to achieve a better test. Until then, the use of the methods based on the above equation have to be treated with caution.

Our final comments concern the uncertainties in the present analysis. In this paper we have developed a method based on $SU(3)$ flavor symmetry to determine the CP violating γ phase. We find that when annihilation contributions are neglected, there are only seven hadronic parameters in the SM related to $B \to PP$ decays. The annihilation contributions are small based on the factorization approximation. If it turns out that they are not small, as some model calculations indicated that the penguin related annihilation contribution A_3^P may be sizeable, one needs to include it in the analysis. However, from Table II one can see that A_3^P does not show up in the $B \to K\pi$ decays, but only in the $B \to \pi\pi$ decays, which is suppressed by small Wilson coefficients. One can also carry out an analysis including A_3^P in the fit when more experimental data become available. Future experimental data with better accuracy will provide more information.

In the estimate of $SU(3)$ breaking effects, we have parametrized the $SU(3)$ breaking effects in a simple form with $C_i(K\pi) = (f_K/f_\pi) C_i(\pi\pi)$. In general, the $SU(3)$ breaking effects may be more complicated. More systematic study of $SU(3)$ breaking effects are needed in order to obtain more accurate determination of the γ phase. But, at any rate, we hope that the method developed here will help to provide useful information about the hadronic matrix elements and also the CP violating γ phase.

In conclusion, in this paper we have developed a method to determine the CP violating γ phase based on the flavor $SU(3)$ symmetry. We find that the present data can already give some constraint on γ and it is consistent with the constraint obtained by using $|\epsilon_K|$, $\Delta m_{B_{d,s}}$, $|V_{ub}/V_{cb}|$, and $\sin 2\beta$ data. We also carried out an analysis combining data from ϵ_K, $\Delta m_{B_{d,s}}$, $|V_{ub}/V_{cb}|$, $\sin 2\beta$, and data from rare charmless hadronic B decays. The combined analysis gives $\gamma = 67°$ for the best-fit value and $43° \sim 87°$ as the 95% C.L. allowed range. Although there are uncertainties in the fit program, the method developed in the present paper can provide useful information about the hadronic matrix elements for rare charmless hadronic B decays and the CP violating phase γ.

ACKNOWLEDGMENTS

X.G.H. thanks P. Chang and D. London for useful discussions. X.G.H., Y.K.H. and J.Q.S. were supported by the National Science Council of ROC under Grant No. NSC89-2112-M-002-058 and NCTS of ROC, and, Y.L.W. and Y.F.Z. were supported by the NSF of China under the Grant No. 19625514.

[1] M. Kobayashi and T. Maskawa, Prog. Theor. Phys. **49**, 652 (1973).
[2] N. Cabibbo, Phys. Rev. Lett. **10**, 531 (1963).
[3] Particle Data Group, D. Groom *et al.*, Eur. Phys. J. C **15**, 1 (2000).
[4] L. Wolfenstein, Phys. Rev. Lett. **51**, 1945 (1983).
[5] S. Mele, Phys. Rev. D **59**, 113011 (1999); A. Ali and D. London, Eur. Phys. J. C **9**, 687 (1999).
[6] F. Parodi, P. Roudeau, and A. Stocchi, Nuovo Cimento A **112**, 833 (1999); F. Caravaglios *et al.*, hep-ph/0002171.
[7] CLEO Collaboration, D. Cronin-Hennessy *et al.*, Phys. Rev. Lett. **85**, 525 (2000).
[8] N. G. Deshpande *et al.*, Phys. Rev. Lett. **82**, 2240 (1999); X.-G. He, W.-S. Hou, and K.-C. Yang, *ibid.* **83**, 1100 (1999); W.-S. Hou, J. G. Smith, and F. Wurthwein, hep-ex/9910014; C. Isola and T. N. Pham, hep-ph/0009210; Y.-L. Wu and Y.-F. Zhou, Phys. Rev. D **62**, 036007 (2000); A. Buras and R. Fleischer, Eur. Phys. J. C **16**, 97 (2000); M. Beneke *et al.*, hep-ph/0007256; Y.-Y. Keum, H.-n. Li, and A. I. Sanda, Phys. Lett. B **504**, 6 (2001).
[9] R. Fleischer and T. Mannel, Phys. Rev. D **57**, 2752 (1998); M. Neubert and J. Rosner, Phys. Lett. B **441**, 403 (1998); Phys. Rev. Lett. **81**, 5076 (1998); X.-G. He, C.-L. Hsueh, and J.-Q. Shi, *ibid.* **84**, 18 (2000); M. Gronau and J. Rosner, Phys. Rev. D **57**, 6843 (1998); N. G. Deshpande and X.-G. He, Phys. Rev. Lett. **75**, 3064 (1995).
[10] M. Savage and M. Wise, Phys. Rev. D **39**, 3346 (1989); **40**, 3127(E) (1989); X.-G. He, Eur. Phys. J. C **9**, 443 (1999); N. G. Deshpande, X.-G. He, and J.-Q. Shi, Phys. Rev. D **62**, 034018 (2000).
[11] M. Gronau *et al.*, Phys. Rev. D **50**, 4529 (1994); **52**, 6356 (1995); **52**, 6374 (1995); A. S. Dighe, M. Gronau, and J. Rosner, Phys. Rev. Lett. **79**, 4333 (1997); L. L. Chau *et al.*, Phys. Rev. D **43**, 2176 (1991); D. Zeppendfeld, Z. Phys. C **8**, 77

(1981).
[12] M. Gronau and D. London, Phys. Rev. Lett. **65**, 3381 (1990); N. G. Deshpande and X.-G. He, *ibid.* **75**, 1703 (1995); M. Gronau and J. Rosner, Phys. Rev. D **57**, 6843 (1998); **61**, 073008 (2000); Phys. Lett. B **482**, 71 (2000); M. Gronau, D. Pirjol, and T.-M. Yan, Phys. Rev. D **60**, 034021 (1999).
[13] X.-G. He, J.-Y. Leou, and C.-Y. Wu, Phys. Rev. D **62**, 114015 (2000).
[14] Y.-F. Zhou *et al.*, Phys. Rev. D **63**, 054011 (2001).
[15] S. Herrlich and U. Nierste, Nucl. Phys. **B419**, 292 (1994); A. J. Buras, M. Jamin, and P. H. Weisz, *ibid.* **B347**, 491 (1990); S. Herrlich and U. Nierste, Phys. Rev. D **52**, 6505 (1995).
[16] T. Draper, Nucl. Phys. B (Proc. Suppl.) **73**, 43 (1999); S. Sharpe, hep-lat/9811006; JLQCD Collaboration, S. Aoki *et al.*, Nucl. Phys. B (Proc. Suppl.) **63A-C**, 281 (1998).
[17] A. Ali and D. London, Z. Phys. C **65**, 431 (1995); Takeo Inami, C. S. Lim, B. Takeuchi, and M. Tanabashi, Phys. Lett. B **381**, 458 (1996).
[18] The LEP B oscillation WG, http://lepbosc.web.cern.ch/LEPBOSC, updated for 30th *International Conference on High Energy Physics*, Osaka, Japan.
[19] J. M. Flynn and C. T. Sachrajda, to appear in *Heavy Flavours*, edited by A. J. Buras and M. Lindner, 2nd ed. (World Scientific, Singapore, 1998); hep-lat/9710057.
[20] H. G. Moser and A. Roussani, Nucl. Instrum. Methods Phys. Res. A **384**, 491 (1997).
[21] BABAR Collaboration, B. Aubert *et al.*, Phys. Rev. Lett. **86**, 2515 (2001); Belle Collaboration, A. Abashian *et al.*, *ibid.* **86**, 2509 (2001).
[22] CDF Collaboration, T. Affolder *et al.*, Phys. Rev. D **61**, 072005 (2000).
[23] ALEPH Collaboration, R. Barate *et al.*, Phys. Lett. B **492**, 259 (2000).
[24] G. Buchalla, A. Buras, and M. Lautenbacher, Rev. Mod. Phys. **68**, 1125 (1996); M. Ciuchini *et al.*, Nucl. Phys. **B415**, 403 (1994).
[25] N. G. Deshpande and X.-G. He, Phys. Lett. B **336**, 471 (1994).
[26] A. Ali, G. Kramer, and C.-D. Lu, Phys. Rev. D **58**, 094009 (1998); **59**, 014005 (1999); A. Datta, X.-G. He, and S. Pakvasa, Phys. Lett. B **419**, 369 (1998); Y.-H. Chen, H.-Y. Cheng, B. Tseng, and K.-C. Yang, Phys. Rev. D **60**, 094014 (1999).
[27] R. Fleischer, Z. Phys. C **62**, 81 (1994); Phys. Lett. B **321**, 259 (1994); **332**, 419 (1994); N. Deshpande, X.-G. He, and J. Trampetic, **345**, 547 (1995); N. G. Deshpande and X.-G. He, Phys. Rev. Lett. **74**, 26 (1995); **74**, 4099(E) (1995).
[28] D. Urner, CLEO TALK 00-33, DPF2000, Columbus, Ohio, 2000; R. Stroynowshi, CLEO Talk 00-30, ICHEP2000, Osaka, Japan, 2000.
[29] T. Iijima, Belle Collaboration, Talk at BCP4, Ise-Shima, Japan, 2001.
[30] A. Hoecker, Paris-Sud, Babar Collaboration, Talk at BCP4, Ise-Shima, Japan, 2001.
[31] CLEO Collaboration, S. Chen *et al.*, Phys. Rev. Lett. **85**, 525 (2000).
[32] D. Melikhov and B. Stech, Phys. Rev. D **62**, 014006 (2000).